JB
Journals.ASM.org

The AbrB2 Autorepressor, Expressed from an Atypical Promoter, Represses the Hydrogenase Operon To Regulate Hydrogen Production in *Synechocystis* Strain PCC6803

Jérémy Dutheil,[a] Panatda Saenkham,[a] Samer Sakr,[a] Christophe Leplat,[a] Marcia Ortega-Ramos,[a] Hervé Bottin,[b] Laurent Cournac,[c,d,e]* Corinne Cassier-Chauvat,[a] and Franck Chauvat[a]

UMR8221, CEA, CNRS, Université Paris Sud, iBiTec-S, LBBC, Gif sur Yvette, France[a]; UMR8221, CEA, CNRS, Université Paris Sud, iBiTec-S, LMB, Gif sur Yvette, France[b]; CEA, UMR7265, iBEB, LBBBM, CEA-Cadarache, Saint-Paul-lez-Durance, France[c]; CNRS, UMR7265, Saint Paul lez Durance, France[d]; and Aix Marseille Université, UMR7265, Saint Paul lez Durance, France[e]

We have thoroughly investigated the *abrB2* gene (sll0822) encoding an AbrB-like regulator in the wild-type strain of the model cyanobacterium *Synechocystis* strain PCC6803. We report that *abrB2* is expressed from an active but atypical promoter that possesses an extended −10 element (TGTAATAT) that compensates for the absence of a −35 box. Strengthening the biological significance of these data, we found that the occurrence of an extended −10 promoter box and the absence of a −35 element are two well-conserved features in *abrB2* genes from other cyanobacteria. We also show that AbrB2 is an autorepressor that is dispensable to cell growth under standard laboratory conditions. Furthermore, we demonstrate that AbrB2 also represses the *hox* operon, which encodes the Ni-Fe hydrogenase of biotechnological interest, and that the *hox* operon is weakly expressed even though it possesses the two sequences resembling canonical −10 and −35 promoter boxes. In both the AbrB2-repressed promoters of the *abrB2* gene and the *hox* operon, we found a repeated DNA motif [TT-(N_5)-AAC], which could be involved in AbrB2 repression. Supporting this hypothesis, we found that a TT-to-GG mutation of one of these elements increased the activity of the *abrB2* promoter. We think that our *abrB2*-deleted mutant with increased expression of the *hox* operon and hydrogenase activity, together with the reporter plasmids we constructed to analyze the *abrB2* gene and the *hox* operon, will serve as useful tools to decipher the function and the regulation of hydrogen production in *Synechocystis*.

Cyanobacteria are ancient photoautotrophic prokaryotes that are regarded as the progenitors of oxygenic photosynthesis (33, 39) and the plant chloroplast (8). Over time, cyanobacteria have evolved as the largest and most diverse groups of bacteria (44) and have colonized most waters and soils of our planet. The hardiness of cyanobacteria is due to their efficient photosynthesis, which uses nature's most abundant resources, solar energy, water, CO_2, and mineral nutrients, to produce a large part of the atmospheric oxygen and organic assimilates for the food chain (52). On a global scale, cyanobacteria fix an estimated 25 gigatons of carbon from CO_2 per year into energy-dense biomass (37, 49). To perform this huge CO_2 fixation, cyanobacteria use 0.2 to 0.3% (49) of the total solar energy, 178,000 TW, reaching the Earth's surface (22). Thus, the amount of energy passing through cyanobacteria exceeds by more than 25 times the energy demand of human society (about 15 TW), roughly 1,000 times the total nuclear energy produced on Earth.

Furthermore, the availability of molecular tools for gene manipulation make cyanobacteria promising "low-cost" microbial cell factories for the carbon-neutral sustainable production of alkanes (10, 41), bioplastics (1), hydrogen (2, 12), and lipids (25, 43), while saving arable soils for crops (50). In light of their tremendous importance, deeper investigation into the mechanisms by which cyanobacteria convey solar energy to the environment is justified. In this frame, investigating the photobiological production of hydrogen by cyanobacteria has both fundamental and applied research values. As the basic research interest, it addresses the paradox of the antagonistic production of oxygen and hydrogen (O_2 inhibits H_2 production). As a biotechnological interest, it may lead to the sustainable production of a high-energy fuel (26), which burns cleanly in producing only water as its by-product.

The pentameric hydrogenase enzyme (HoxEFUYH; Hox for hydrogen oxidation) of cyanobacteria produces H_2 through the reversible reaction $2\,H^+ + 2\,e^- \leftrightarrow H_2$, which uses NAD(P)H as the source of electrons originating from photosynthesis and/or sugar catabolism, as well as a nickel-iron cluster and several iron-sulfur centers as redox cofactors (5). The Hox enzyme has been studied mostly in the best-characterized unicellular cyanobacterium, *Synechocystis* strain PCC6803 (here designated *Synechocystis*), which harbors a small genome (less than 4 Mb [see CyanoBase, http://genome.kazusa.or.jp/cyanobase/]) that is easily manipulable (14, 29, 38). The active Hox enzyme, matured by the HoxW protease (47) and assembled using the six-subunit HypABCDEF complex (5), has been recently characterized as a truly bidirectional enzyme with a bias toward H_2 production (30). The five genes *hoxEFUYH* are clustered in a octacistronic operon that also contains three open reading

Received 13 April 2012 **Accepted** 27 July 2012
Published ahead of print 3 August 2012
Address correspondence to Franck Chauvat, franck.chauvat@cea.fr.
* Present address: Laurent Cournac, UMR Eco&Sols, IRD, CIRAD, INRA, Supagro, Montpellier, France.
J.D., P.S., and S.S. contributed equally to this work.
Supplemental material for this article may be found at http://jb.asm.org/.

doi:10.1128/JB.00543-12

TABLE 1 Characteristics of plasmids used in this study

Plasmid use and name	Relevant feature(s)	Reference
Targeted deletion of *abrB2* in *Synechocystis*		
pGEMT	AT overhang Amp^r cloning vector	Promega
pUC4K	Source of Km^r marker gene	Pharmacia
pΔsll0822	pGEMT with *Synechocystis sll0822* flanking sequences, with *sll0822* coding sequence (from bp 7 to 384) replaced by SmaI site	This study
pΔsll0822::Km^r	pΔsll0822 with Km^r marker inserted into unique SmaI site	This study
High-level expression of *abrB2* in *Synechocystis*		
pFC1	Replicating plasmid for heat-inducible gene expression in *Synechocystis*	32
pSll0822	pFC1 with *sll0822* CS cloned between NdeI-EcoRI sites	This study
Analysis of *hox* and *abrB2* promoters in *Synechocystis*		
pSB2A	Km^r Sm^r/Sp^r replicative promoter probe plasmid harboring unique SnaBI site in front of its promoterless *cat* reporter gene	27
pPS1	Km^s derivative of pSB2A generated after cleavage with NsiI and religation	This study
pJD1	*hox* PR[a] (bp −794 to +173 relative to TSS) cloned at SnaBI site of pPS1	This study
pJD2	*hox* PR (bp −522 to +173 relative to TSS) cloned at SnaBI site of pPS1	This study
pJD3	*hox* PR (bp −403 to +173 relative to TSS) cloned at SnaBI site of pPS1	This study
pJD4	*hox* PR (bp −170 to +173, relative to TSS) cloned at SnaBI site of pPS1	This study
pPS2	*abrB2* PR (bp −75 to +88 relative to TSS) cloned at SnaBI site of pSB2A	This study
pPS2 m-8	pPS2 harboring T→G mutation at −8 position relative to TSS	This study
pPS2 m-13	pPS2 harboring T→G mutation at −13 position relative to TSS	This study
pPS2 m-15	pPS2 harboring T→G mutation at −15 position relative to TSS	This study
pPS2 m-4746	pPS2 harboring TT→GG mutation at positions −47 to −46 relative to TSS	This study
Production of AbrB2 in *E. coli*		
pET14b	Amp^r *E. coli* plasmid for production of 6×His-tagged proteins	Novagen
pSS1	pET14b plasmid with sll0822 CS cloned between NdeI and BamHI sites	This study

[a] PR, promoter region.

frames of unknown function. This operon is weakly expressed as a polycistronic transcript, which initiates 168 bp upstream of the start codon of the proximal *hoxE* gene (15, 35). The transcriptional regulation of the *hox* operon is complex in responding to various environmental conditions (21), and it involves at least three proteins (36). The LexA-related protein Sll1626, which appears to regulate carbon assimilation rather than DNA repair (9), was found to activate the transcription of the *hox* genes through binding to the promoter of the *hox* operon (15, 35). In addition, two AbrB-like regulators, which have their putative DNA-binding domain in the C-terminal region instead of in the usual N-terminal region, as occurs in other prokaryotes (19), were found to operate in *hox* regulation. In *Bacillus subtilis*, the AbrB regulator is implicated in the regulation of about 100 genes involved in sporulation, biofilm formation, antibiotic production, and development of competence for DNA uptake, but its promoter recognition consensus sequence and mode of interaction with DNA remain unclear (6). In *Synechocystis*, the AbrB1 (Sll0359) protein was found to be indispensable to cell life in the wild-type (WT) strain (34) and the glucose-tolerant mutant (19). Furthermore, AbrB1 was shown to bind to the promoter region of its own gene and to activate transcription of the *hox* operon through binding to the *hox* operon promoter (34). In contrast, AbrB2 (Sll0822) was studied only in the glucose-tolerant strain, which possesses several specific mutations that may interfere, at least indirectly, with the studied process (20). In the glucose-tolerant mutant, AbrB2 appeared to (i) be dispensable to cell life, (ii) bind to the promoter regions of its own gene and of other genes involved in nitrogen and carbon assimilations (19, 24, 51), and (iii) negatively influence expression of the *hox* operon via an unknown mechanism (19).

In this study, we thoroughly investigated the function and regulation of the *abrB2* gene in the wild-type strain of *Synechocystis*, because it is the organism that actually occurs in nature. We demonstrate that *abrB2* is expressed from an atypical promoter that possesses an extended −10 element to compensate for the absence of a −35 box. Furthermore, we demonstrate through gene deletion and overexpression that AbrB2 represses its own gene, as well as the *hox* operon, which is of biotechnological interest. We think that our *abrB2*-deleted mutant with an improved hydrogenase activity and healthy growth, and also the reporter plasmids we constructed to analyze the promoters of the *abrB2* gene and the *hox* operon, will serve as useful tools to decipher the regulation and the function of the hydrogen production machine in cyanobacteria.

MATERIALS AND METHODS

Bacterial strains and culture conditions. *Synechocystis* PCC6803 was grown at 30°C or 39°C (depending on the strain) under continuous white light (2,500 lx, 31.25 μE m^{-2} s^{-1}) on BG11 medium (40) enriched with 3.78 mM Na_2CO_3 (9).

E. coli strains used for gene manipulations (TOP10; Invitrogen), production of recombinant proteins [BL21(DE3); Novagen], or conjugative transfer to *Synechocystis* (CM404; [31]) of replicative plasmids (Table 1) derived from our temperature-controlled expression vector pFC1 (32) were grown on LB medium at 30°C (CM404 and TOP10 harboring pFC1 derivatives) or 37°C [TOP10 and BL21(DE3)]. Antibiotic selection was as follows: for *E. coli*, ampicillin (Ap) at 100 μg ml^{-1} or 50 μg ml^{-1}, kanamycin (Km) at 50 μg ml^{-1}, and spectinomycin (Sp) at 100 μg ml^{-1} for *E.*

coli; for *Synechocystis*, Km at 50 to 300 μg ml^{-1}, Sp at 5 μg ml^{-1}, and streptomycine (Sm) at 5 μg ml^{-1}.

Construction of the DNA cassette for targeted deletion of the *Synechocystis abrB2* gene. The two regions of *Synechocystis* DNA (each about 300 bp in length) flanking the *abrB2* (sll0822) protein coding sequence (CS) were independently amplified by PCR, using the primers sll0822M-Fw and sll0822R4 for the upstream region and sll0822M-Rv and sll0822A4 for the downstream region (see Table S1 in the supplemental material). These two DNA regions were fused through standard PCR-driven overlap extension (17) in a single DNA segment harboring a SmaI restriction site in place of the *abrB2* CS. After cloning in pGEMT (Table 1), the resulting plasmid was opened at the unique SmaI site, where we cloned the Km^r resistance cassette (a HincII fragment of pUC4K) in the same orientation as the *abrB2* CS it replaced. The resulting Δsll0822::Km^r deletion cassette was verified by PCR and nucleotide sequencing (BigDye kit; ABI, Perkin-Elmer).

Construction of the vector for high-level expression of the *abrB2* gene in *Synechocystis*. Our temperature-controlled expression vector pFC1, which replicates autonomously in *E. coli* and several cyanobacteria (32), was used for high-level expression of the *Synechocystis abrB2* gene. pFC1 harbors the λ*cI*857 temperature-sensitive repressor-encoding gene that tightly controls the activity of the otherwise-strong λ*pR* promoter located downstream, which is followed by the λ*cro* ribosome-binding site (5′-AGGA-3′) and ATG start codon (in bold) embedded within the unique NdeI restriction site (5′-CAT**ATG**-3′) for in-frame fusion of protein coding regions. The *abrB2* CS was PCR amplified from *Synechocystis* DNA, using specific primers (sll0822FL1 and sll0822FL2 [see Table S1 in the supplemental material]), which flanked the *abrB2* CS between unique NdeI and EcoRI restriction sites, for cloning into pFC1, opened with the same enzymes. The Smr/Spr resulting plasmid, pSll0822, for high-level expression of *abrB2* at 39°C was verified by PCR and nucleotide sequencing (BigDye kit; ABI Perking Elmer).

RNA isolation. Aliquots of 200 ml of mid-log-phase cultures (2.5×10^7 cells ml^{-1}) were rapidly harvested by vacuum filtration (less than 1 min), resuspended in 4 ml of 50 mM Tris 50 (pH 8), 5 mM EDTA, immediately frozen in an Eaton press chamber cooled in a dry ice and ethanol bath, and disrupted (250 MPa). RNA was extracted and purified with the Qiagen RNeasy kit as we have previously described (18) and then treated with 20 U of DNase I, RNase-free (Applied Biosystems) for 30 min at 37°C. RNA concentration and purity (A_{260}/A_{280} ratio, >1.9) were determined with a Nanodrop apparatus (Thermo Scientific) and migration on an agarose gel to verify the absence of RNA degradation. The absence of contaminant DNA was verified with the *Taq* DNA-dependent DNA polymerase (Invitrogen) using primers specific to the control gene *rnpB* (see Table S1 in the supplemental material).

RT-PCR and quantitative PCR. cDNAs were synthesized from 5 μg of total RNA by using Moloney murine leukemia virus reverse transcriptase (RT; Invitrogen). Samples were then incubated for 20 min at 37°C with 4 U RNase H (Applied Biosystems) to eliminate RNA templates, and the cDNA concentration was measured with Nanodrop apparatus adjusted to 1 μg μl^{-1} by dilution in H_2O. Quantitative PCR (qPCR) assays of the expression levels of the studied genes and the well-known constitutive control gene *rnpB* (see Table S1 in the supplemental material) were performed with Mesa Green qPCR MasterMix Plus for SYBR assay (RT-SYS2X-03+WOU; Eurogentec) according to the manufacturer's instructions. The gene-specific primers were chosen so as to generate DNA fragments of similar length, between 199 bp and 234 bp. Each reaction was performed in a 50-μl reaction mixture containing 5 ng cDNA, 0.04 μM specific primer, 1× Mesa Green qPCR MasterMix Plus buffer, and 2 mM $MgCl_2$ in an iCycler iQ 96-well reaction plate covered with adhesive film (Bio-Rad). Samples were incubated in an iQ5 multicolor real-time PCR detection system (Bio-Rad) for 2 min at 50°C, 2 min at 95°C, and 45 cycles of 15 s at 95°C and 1 min at 60°C. Each assay was performed in triplicate, allowing the mean threshold cycle value (C_T) to be calculated from standard curve by using the iQ5 optical system software (Bio-Rad). Each gene-specific standard curve was made by 4-fold serial dilution of wild-type strain cDNA (ranging from 312.5 to 0.3 ng) compared to the log input cDNA concentration for each primer (data not shown). For each primer tested, the regression value (ΔC_T versus cDNA concentration) was less than 0.1, indicating approximately equal amplification efficiencies. Then, for each studied gene, the C_T value was converted to the gene copy number per ng of template cDNA.

Determination of the TSS of sll0822 by 5′-random amplification of cDNA ends (5′-RACE). Aliquots of 25 μg of total RNAs of the *Synechocystis* WT strain were treated with shrimp alkaline phosphatase (SAP), which does not affect the 5′-triphosphate extremity of full-length mRNAs but dephosphorylates the 5′-monophosphate end of degraded RNA. Then, RNAs were treated with tobacco acid pyrophosphatase (TAP; Epicentre) to convert the 5′-triphosphate extremity of full-length mRNA into the 5′-monophosphate without modifying the 5′-OH end of degraded RNA. The 5′-monophosphate extremity of the full-length mRNAs was ligated to an RNA anchor (see Table S1 in the supplemental material) with the T4 RNA ligase (Invitrogen). The resulting chimeric RNAs were reverse transcribed with SuperScript II (Invitrogen) and the sll0822 gene-specific primer sll0822P1 (see Table S1). This first strand of cDNA was amplified by PCR using both the DNA anchor at the 5′ extremity and the sll0822P1 primer at the 3′ side. The resulting DNA was sequenced (BigDye kit; ABI Perkin-Elmer) to identify the first sll0822 nucleotide located immediately downstream of the DNA anchor, which is the sll0822 transcription start site (TSS) (see Fig. S1 in the supplemental material).

Construction of transcriptional fusions to the *cat* reporter gene and the CAT assay. The studied promoter regions were amplified by PCR with specific oligonucleotides designed to introduce blunt-ended restriction sites in a way that allowed the elimination of all nucleotide substitutions upon restriction cleavage (see Table S1 in the supplemental material). These promoters were cloned in the unique SnaBI site preceding the promoterless *cat* (chloramphenicol acetyltransferase) reporter gene of our promoter probe vector pSB2A or of its Km^s derivative, pPS1 (Table 1), which replicate in *Synechocystis* with the same copy number as the chromosome (27). Site-directed mutagenesis of the sll0822 promoter was done through standard PCR-driven overlap extension (17) using specific mutagenic primers (see Table S1) and the forward and reverse primers SnaBIFW22 and SnaBIRV22. The sequence of each promoter insert was verified, before and after propagation in *Synechocystis*. Then, 1×10^9 to 2×10^9 cells grown on standard plates to mid-log phase were rapidly harvested and disrupted with a chilled Eaton press prior to CAT assay (28).

AbrB2 production and purification from *E. coli*. The *abrB2* coding sequence was PCR amplified from *Synechocystis* DNA with the primers abrB2-NdeI-Fw and abrB2-BamHI-Rv (see Table S1 in the supplemental material), digested with both NdeI and BamHI, and cloned into the pET14b plasmid opened with the same enzymes for in-frame fusion to the 6×His tag. The resulting plasmid, pSS1 (Table 1), was introduced into *E. coli* BL21(λDE3), which was grown to mid-log phase prior to the addition of 0.5 mM isopropyl-β-D-thiogalactopyranoside (IPTG) for 3 h to produce the 6×His-AbrB2 protein. Cells were harvested by centrifugation at 7,000 rpm for 5 min at 4°C, suspended in buffer A (30 mM Tris-HCl [pH 7.5], 400 mM NaCl, 20 mM imidazole) containing 2 mg/ml lysozyme (Sigma-Aldrich), and incubated for 1 h on ice. After sonication on ice (6 pulses, 20 s each) and centrifugation (13,000 rpm for 30 min at 4°C), cell lysates were loaded onto a 1 ml Ni-nitrilotriacetic acid–agarose column (Qiagen) preequilibrated with buffer A and washed with 10 bed volumes of 30 mM imidazole in buffer A. The proteins eluted with 300 mM imidazole in buffer A were analyzed by SDS-PAGE. AbrB2-containing fractions were pooled, concentrated with Amicon Ultra centrifugal filter devices (Millipore), diluted in buffer B (30 mM Tris-HCl [pH 7.5], 100 mM NaCl), loaded onto a heparin column (GE Healthcare) preequilibrated with buffer B, and washed with 10 bed volumes of buffer B. AbrB2 was eluted with a linear 0-to-500 mM NaCl gradient in 30 mM Tris (pH 7.5), and the AbrB2-enriched fractions were pooled, concentrated, and stored

in 30 mM Tris (pH 7.5), 400 mM NaCl. AbrB2 protein purity, estimated by SDS-PAGE, was greater than 95%.

Electromobility shift assays (EMSAs). The studied promoter regions were PCR amplified from *Synechocystis* DNA with specific primers (see Table S1 in the supplemental material) purified, 3′-end-labeled with digoxigenin (DIG gel shift kit, 2nd generation; Roche), incubated with AbrB2, migrated on a Novex 6% DNA retardation gel (Invitrogen), blotted on a positively charged nylon membrane (Roche) with a semidry transfer apparatus (Apelex), and cross-linked onto the membrane with a 2-min UV-C (254 nm) exposure (Stratalinker). The DNA bands were revealed with anti-DIG antibodies by chemiluminescence, using Hyperfilm ECL (Amersham Pharmacia) and Kodak developer.

Hydrogenase activity measurements. Hydrogenase activities were measured by two standard methods. First, hydrogen evolution was measured with a modified Clark-type electrode (Hansatech, United Kingdom) (48) as described previously by some of us (46). A total of 2.5×10^7 cells (1-ml culture at an optical density at 580 nm of 1) were harvested by a 5-min centrifugation at 5,000 rpm, resuspended in 25 μl of 50 mM Tris-HCl (pH 7.5) buffer, and introduced into 500 μl of a solution containing 50 mM Tris-HCl (pH 7.5), 20 mM Na-dithionite, and 5 mM methylviologen as the electron donor to hydrogenase. Calibration was performed using the amplitude of the electrical signal from the electrode in the presence of an aliquot of H_2-saturated water as a concentration reference. Second, hydrogenase activity (the H/D exchange rate of labeled dihydrogen) was determined by membrane-inlet mass spectrometry (MIMS) on cell suspensions, as we have described previously (3, 7).

RESULTS

The *abrB2* gene is dispensable to the viability of the wild-type strain of *Synechocystis*. In the framework of our long-term interest in gene regulation, we have investigated the AbrB2 regulator (Sll0822 in CyanoBase) of the model cyanobacterium *Synechocystis*. Therefore, we constructed the Δ*abrB2*::Km^r deletion cassette (Table 1), in which the complete coding sequence for the 129-amino-acid AbrB2 protein has been deleted and replaced by a transcription terminatorless Km^r marker for selection (Fig. 1A). After transformation in the WT strain of *Synechocystis*, we verified through PCR (Fig. 1B) and DNA sequencing (data not shown) that the Km^r marker had properly replaced the *abrB2* gene in all copies of the polyploid chromosome (13, 23). We also verified through RT-PCR and quantitative RT-PCR that the mutant completely lacked *abrB2* mRNA (data not shown). These data, together with the fact that the Δ*abrB2*::Km^r mutant grows as healthy as the WT strain (Fig. 1C), showed that the AbrB2 protein is dispensable to the growth of *Synechocystis*. This finding is consistent with, but not identical to, the previous observation that the insertion of the Km^r marker at 177 bp downstream of the ATG start codon of *abrB2* (possibly leading to the synthesis of an aberrant protein) did not impair the viability but strongly reduced the growth rate of the glucose-tolerant mutant of *Synechocystis* (19), which has several specific mutations compared to the WT strain (20), i.e., the organism actually occurring in nature.

AbrB2 negatively regulates expression of its own gene through binding to its own promoter. The *Synechocystis* AbrB2 protein was translationally fused to the 6×His tag for facile purification from recombinant *E. coli* cells to near homogeneity through nickel affinity chromatography. Then, this 6×His-AbrB2 protein was used for an EMSA to determine its ability to bind the DIG-labeled, 163-bp-long promoter region (Fig. 2) shared by the divergently transcribed genes *abrB2* and slr0846 (Fig. 1). We found that AbrB2 binds on this 163-bp full promoter region, in agreement with a previous observation (19), and on the two sub-

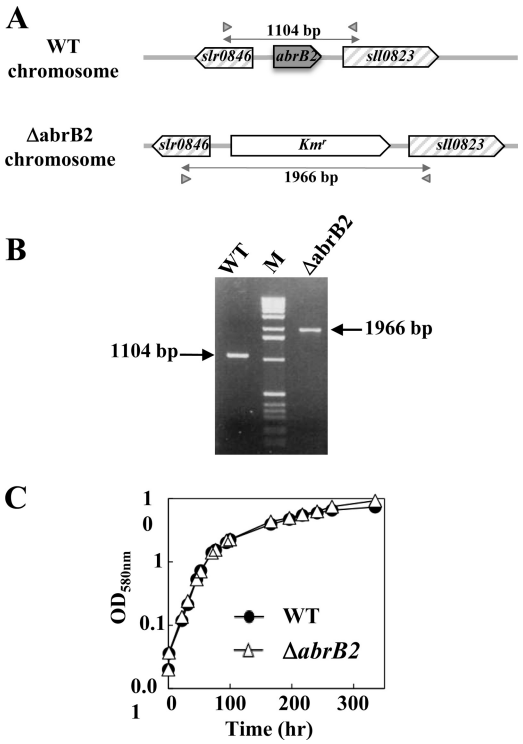

FIG 1 Influence of the AbrB2 regulator on growth of *Synechocystis* under standard conditions. (A) Schematic representation of the *abrB2* chromosome locus in the WT strain (see CyanoBase) and the *abrB2*-deleted mutant (Δ*abrB2*::Km^r) constructed in this study. The genes are represented by boxes pointing in the direction of their transcription. The PCR primers specific to the slr0846 and sll0823 genes are represented by the small gray triangles, and the sizes of the products they generated upon amplification of the *abrB2* chromosome locus of the WT (1,104 bp) and *abrB2*-deleted (Δ*abrB2*::Km^r; 1,966 bp) chromosomes are indicated by double arrows. (B) UV light image of the agarose gel, showing the 1,104-bp and 1,966-bp PCR product typical of the WT and *abrB2*-deleted chromosomes, respectively; the results show that the *abrB2*-deleted mutant harbors no WT copies of the chromosome. (C) Growth of the WT strain and the Δ*abrB2* mutant (this experiment was repeated three times and yielded statistical deviations too small to be represented).

fragments tested here (Fig. 2); thus, the promoter region contains several AbrB2-binding motifs (see below). As negative-control experiments, we verified the absence of binding of (i) AbrB2 on a heterologous (noncyanobacterial) DNA (see Fig. S2 in the supplemental material) and (ii) the bovine serum albumin (BSA) protein on the *abrB2* promoter DNA (see Fig. 5B, below; see also Fig. S2 in the supplemental material). The obvious interpretation of the binding of AbrB2 on its own promoter is that AbrB2 is an autoregulator. To test this hypothesis, we performed a thorough *in vivo* analysis of the *abrB2* promoter by using our promoter probe vector, which harbors the promoterless *cat* reporter gene for promoter analysis and replicates autonomously in *Synechocystis* with a similar copy number as the chromosome (27). We cloned the whole intergenic region (163 bp) between the divergently transcribed genes *abrB2* and slr0846 in front of the *cat* reporter gene, and we selected the p*abrB2-cat* reporter plasmid (pPS2 [Table 1]) expressing the *cat* gene from the *abrB2* promoter. This p*abrB2-cat* plasmid (Table 1) was introduced in both the WT strain and our *abrB2* deletion mutant (Δ*abrB2*::Km^r), where it replicated stably, as expected (data not shown). The level of *cat* expression driven by the *abrB2* promoter in the WT strain (44 CAT units [Fig. 3A]) was

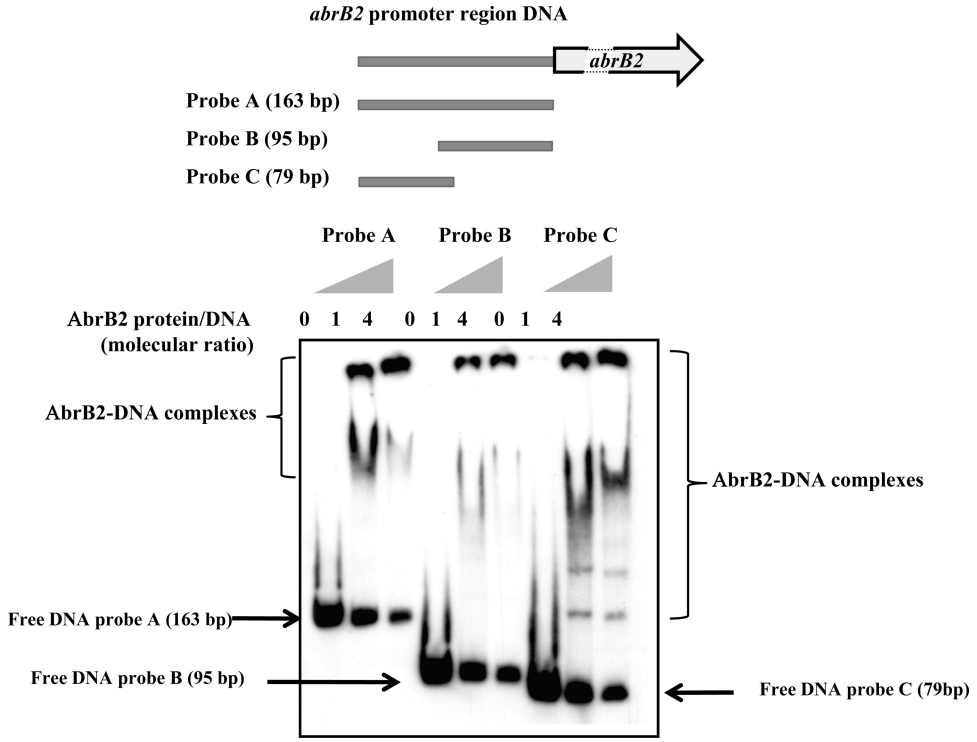

FIG 2 Electrophoretic migration shift assay of binding of the AbrB2 regulator to the promoter region of its own gene. (Top) Schematic representation of the *abrB2* gene, showing its 163-bp promoter region (gray line) and its protein-coding sequence (boxed arrows), which is interrupted (dashed lines) for the sake of size limitation. The positions and sizes of the three DNA fragments of the *abrB2* promoter region used as targets for AbrB2 binding are indicated as probes A, B, and C. (Bottom) Analysis of the electrophoretic mobility of the DIG-labeled segments of the *abrB2* promoter region, following incubation with increasing amounts of purified 6×His-AbrB2 protein. Arrows and regions delineated by braces indicate the positions of the free DNA probes and the retarded DNA-protein complexes, respectively.

similar to that directed by the other promoters we previously analyzed (references 11 and 45 and references therein). This finding indicates that the *abrB2* promoter has an average strength. As the usual control, we verified that the empty promoter probe vector with no promoter insert produced no CAT activity. Very interestingly, the *abrB2* promoter was found to be more active (about 3-fold) in the *abrB2* deletion mutant (131 CAT units), i.e., in the absence of the AbrB2 protein, thereby demonstrating that AbrB2 negatively regulates the expression of its own gene. Collectively, our data unambiguously demonstrate, for the first time, that AbrB2 is an autorepressor.

The core promoter of the *abrB2* gene possesses an "extended −10 element" which compensates for the absence of a −35 box. Using the classical 5′-RACE technique (42), which has performed well in our hands (11, 45), we mapped the TSS of *abrB2*. It is the G nucleotide located 87 bp upstream of the ATG start codon (see Fig. S1 in the supplemental material). Then, we performed a mutational analysis of the *abrB2* promoter to identify its *cis*-acting elements. We studied the 5′-TAatAT-3′ hexamer (lowercase letters indicate nucleotides that are not widely conserved) matching the canonical −10 box of σ^{70}-type *Escherichia coli* promoters (16) with regard to both sequence (5′-TAatAT-3′) and its position (−13 to −8) from the TSS, the above-mentioned G nucleotide we used as the origin of distance (noted as +1 [see Fig. S1 in the supplemental material]). As anticipated, this 5′-TAatAT-3′ *abrB2* element behaves as a −10 promoter box, as it is crucial to transcription. Indeed, transversion mutagenesis of either its presumably important T nucleotides (5′-TAatAT-3′ to 5′-GAatAT-3′ and 5′-TAatAT-3′ to 5′-TAatAG-3′) completely abolished *abrB2* promoter activity (Fig. 3A; reporter plasmids pPS2m-13 and pPS2m-8, respectively), as we previously observed with the −10 box of several *Synechocystis* promoters (references 11 and 45 and references therein). In the *abrB2* promoter, we also noticed the presence of a 5′-TTGAac-3′ motif, resembling a canonical −35 box (16) in sequence (5′-TTGACA-3′) but not position (28 bp instead of 17 ± 1 bp, the usual spacing distance from the −10 box). We mutagenized this 5′-TTGAac-3′ *abrB2* element and found that it was not crucial to promoter activity (Fig. 3A, pPS2m-4746 plasmid), unlike a −35 promoter box. Instead, this *abrB2* 5′-TTGAac-3′ motif appeared to negatively influence the activity of the *abrB2* promoter (Fig. 3A). Then, having in mind that the absence of a −35 promoter box can be compensated by the presence of an "extended −10 box" mediating all contacts with the RNA polymerase σ^{70} factor (4), we mutagenized the upstream T of the presumptive extended −10 box, 5′-TGTAATAT-3′ of the *abrB2* promoter. As anticipated, this mutation (5′-TGTAATA T-3′ to 5′-GGTAATAT-3′ decreased the *abrB2* promoter activity (Fig. 3A, pPS2m-15 plasmid), similarly to what we found in the case of the "extended −10 box" of the *secA* promoter (28). In agreement with its crucial importance for *abrB2* transcription, we found the "extended −10 box," 5′-TGTAATAT-3′, to be highly conserved in the promoter region of the *abrB2* genes from other cyanobacteria (Fig. 3B). Collectively, our data indicate that the *abrB2* promoter possesses an extended −10 element to compen-

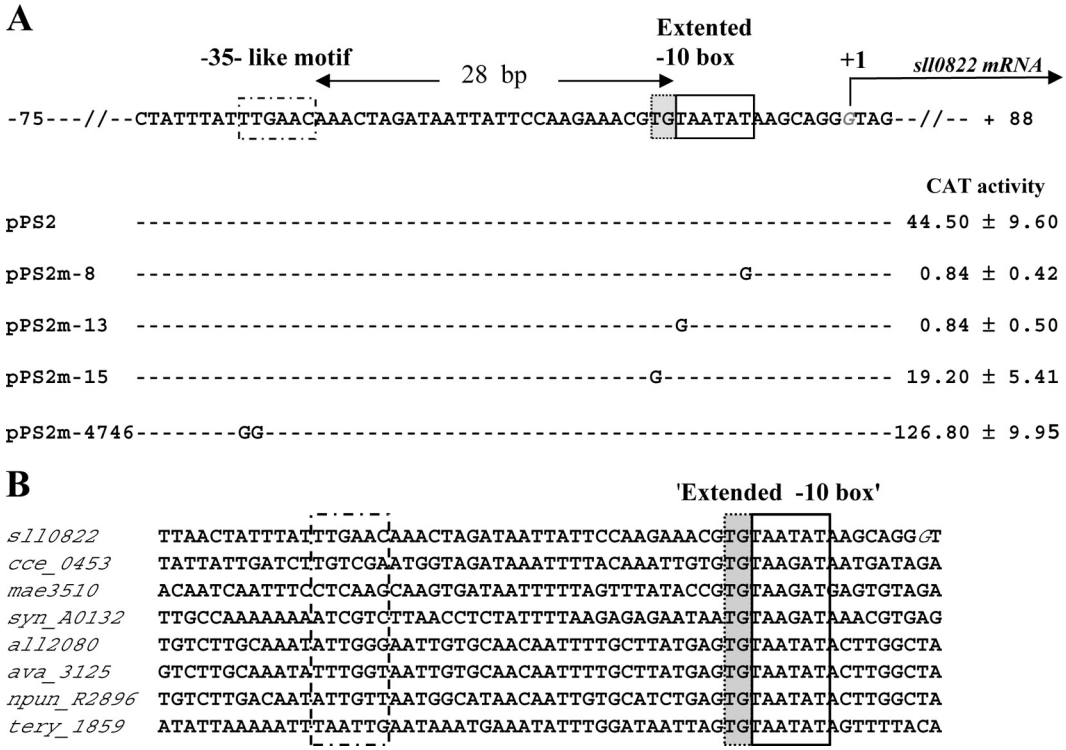

FIG 3 Mutational analysis in *Synechocystis* of the *abrB2* promoter transcriptionally fused to the *cat* reporter gene of our replicative promoter probe vector. (A) Sequence alignment of the nontranscribed DNA strand of the WT (pPS2 reporter plasmid) and mutant (pPS2m reporter plasmids) *abrB2* promoters. Sequence resembling the −35 and extended −10 promoter elements are boxed, and the origin of transcription (+1; G nucleotide in italics) that we mapped in this study (see Fig. S1 in the supplemental material) is indicated by the bent arrow. Nucleotide substitutions in the mutant promoters (m-8, m-13, m-15, and m-4746) are shown in uppercase letters, while the conserved nucleotides are indicated by dashed lines. For each reporter strain, the CAT activity is the mean value of three measurements performed on two independent cellular extracts; 1 CAT unit = 1 nmol of chloramphenicol acetylated/min/mg of protein. (B) Sequence alignments of the *abrB2* promoter regions from various cyanobacteria resembling *Synechocystis* in that their *abrB2* gene is divergently transcribed with an opposite gene. Besides *Synechocystis* PCC6803 (sll0822), these cyanobacteria are as follows: *Cyanothece* ATCC 51142 (cce_0453), *Microcystis aeruginosa* NIES-843 (mae_35130), *Nostoc* PCC 7120 (all2080), *Anabaena variabilis* ATCC 29413 (ava_3125), *Nostoc punctiforme* PCC 73102 (npun_R2896), and *Trichodesmium erythraeum* ISM101 (tery_1859). The positions of the conserved extended −10 promoter element and of the nonconserved sequence resembling a −35 element in *Synechocystis* are indicated by boxes.

sate for the absence of a −35 box and that these features are conserved in other cyanobacteria.

AbrB2 negatively regulates both the expression and the hydrogenase activity of the *hoxEFUYH* operon. We used quantitative RT-PCR to analyze the influence of the AbrB2 regulator on the transcript abundance of the eight-gene *hox* operon, namely, sll1220 (*hoxE*), sll1221 (*hoxF*), sll1222, sll1223 (*hoxU*), sll1224 (*hoxY*), ssl2420, sll1225, and sll1226 (*hoxH*). Therefore, total RNAs were isolated from WT and *abrB2*-deleted (Δ*abrB2*::Km^r) cells growing under standard conditions and were subsequently hybridized with the gene-specific RT-PCR primers (see Table S1 in the supplemental material) designed to amplify a segment of each of the eight protein-coding sequences of the *hox* operon (Fig. 4A). All eight transcripts were found to be at least 2.5-fold more abundant in the *abrB2*-deleted mutant than in the WT strain (Fig. 4B). As a negative control, we verified the absence of *abrB2* transcripts in the *abrB2*-deleted mutant (data not shown). Together, these data show that AbrB2 negatively regulates the *hox* operon in WT cells of *Synechocystis*, in agreement with what was observed in the glucose-tolerant mutant (19). From these results one can anticipate that the hydrogenase activity should increase in response to the absence of the AbrB2 regulator. Therefore, we used the two classical methods to measure the level of hydrogenase activity, which appeared to be at least 2-fold higher in our *abrB2*-deleted mutant than in the WT strain (Fig. 4B), as expected. To confirm that AbrB2 negatively regulates the expression of the *hox* operon and the activity of the hydrogenase in *Synechocystis*, we constructed an *abrB2* overexpression mutant, as follows. We cloned the *abrB2* protein-coding sequence into our temperature-controlled expression vector, pFC1, which replicates autonomously in cyanobacteria and tightly controls the production of the studied protein according to the growth temperatures, i.e., no production at 30°C and strong production after 24 h of induction at 39°C (32, 38). The resulting pSll0822 plasmid was introduced by conjugative transfer in *Synechocystis* cells, which were transferred for 24 h at 39°C to verify the strong induction of *abrB2* expression (27-fold [data not shown]) and the concomitant downregulation (by at least 2-fold) of *hox* expression and hydrogenase activity (Fig. 4C). Collectively, these results demonstrate that AbrB2 negatively regulates expression of the *hox* operon and activity of the hydrogenase in *Synechocystis*.

AbrB2 negatively regulates the activity of the *hox* operon promoter. We used our promoter probe vector to test whether AbrB2 negatively controls the promoter of the *hoxEFUYH* operon. As *Synechocystis* promoters can be complex in harboring several *cis*-acting regulatory elements (references 9 and 45 and

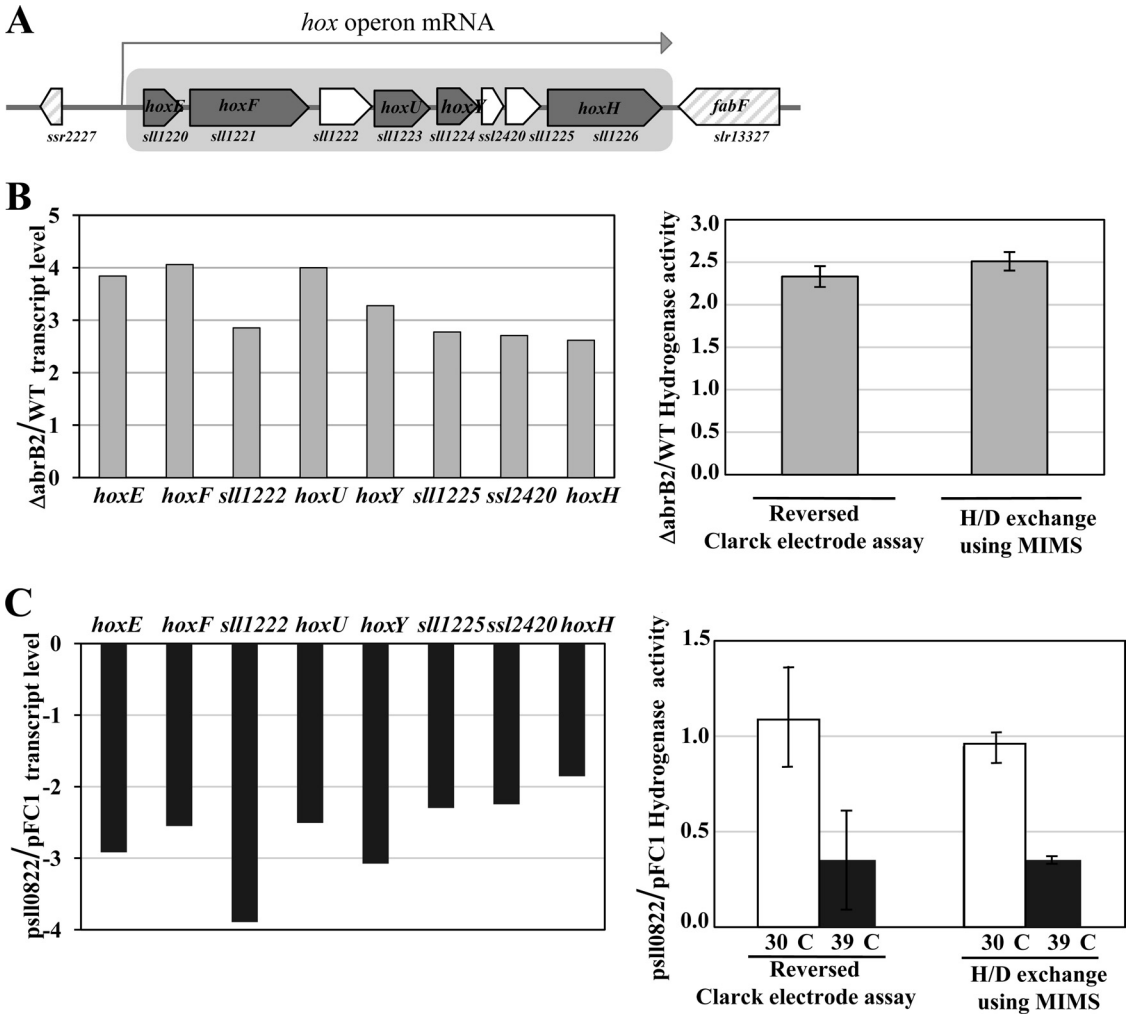

FIG 4 Analysis of expression of the hydrogenase-encoding genes and of hydrogenase activity in various strains of *Synechocystis* harboring a wild-type *abrB2* gene (WT), a deletion of *abrB2* (Δsll0822::Km^r), a plasmid (psll0822) for high-level expression of *abrB2* inducible by 24 h of growth at 39°C, or the empty expression vector (pFC1). All results are expressed as means ± standard deviations of the data obtained after 3 to 6 biological repetitions of each assay. (A) Schematic representation of the locus of the octacistronic *hox* operon. The genes are represented by boxes pointing in the direction of their transcription; boxes are gray in the case of the *hox* genes. (B, left) Histogram plots of the ratios of transcript abundance (measured by quantitative real-time PCR) of each gene of the octacistronic *hox* operon in the *abrB2*-deleted mutant over the WT strain. (Right) Histogram representation of the hydrogenase activity ratios in Δ*abrB2* over WT cells measured with the MIMS assay and a reversed Clark-type electrode, as indicated. (C, left) Histograms showing the transcript level ratios of each gene of the octacistronic *hox* operon, in cells propagating psll0822 over those propagating pFC1, which were all grown for 24 h at 39°C prior to qRT-PCR analysis. (Right) Histogram representation of the hydrogenase activity ratios of cells propagating psll0822 over those propagating pFC1, before (white rectangles) or after (black rectangles) 24 h of growth at 39°C, prior to MIMS and Clark-type electrode assays, as indicated.

references therein), we cloned in our vector the whole *hox* promoter region occurring between the opposite genes *hoxE* and ssr2227, along with the first 5 bp of their protein-coding sequences (Fig. 5A). This 967-bp *hox* promoter region extends from −794 to +173 nucleotides relative to the transcription start site (the A nucleotide mapped by other workers [15, 35], which we used as the origin of distance). Our *hoxprom-cat* reporter plasmid (pJD1 [Fig. 5A]) weakly expressed the *cat* gene in *Synechocystis* (less than 1 CAT unit), thereby indicating that the *hox* promoter was weakly active, in agreement with the low abundance of *hox* transcripts (34). However, the low activity of the *hox* promoter seemed at variance with the occurrence in this promoter of the two sequences resembling canonical promoter boxes, −35 (TTGctc) and −10 (TAacAa), which are located at correct distances from each other (18 bp) and from the transcription start site (7 bp). This apparent discrepancy prompted us to speculate that the AbrB2 regulator, which negatively regulates the expression of the *hox* operon (Fig. 4), operates at the level of *hox* promoter activity. To verify this hypothesis, we introduced the *hox-cat* reporter plasmid pJD1 in the *abrB2*-deleted mutant (Δ*abrB2*::Km^r), and *cat* expression was found to be much higher (about 13 CAT units [Fig. 5A]) than in WT cells, as expected.

Then, to meaningfully examine the EMSA analysis of the binding of AbrB2 on the *hox* promoter, we subcloned the long *hox* regulatory region (967 bp) in our promoter probe vector. Then, we serially deleted the 5′ end of the *hox* regulatory region while keeping its 3′ end intact, because such promoter downstream regions can contain negative *cis*-acting elements (9, 28, 45). As ex-

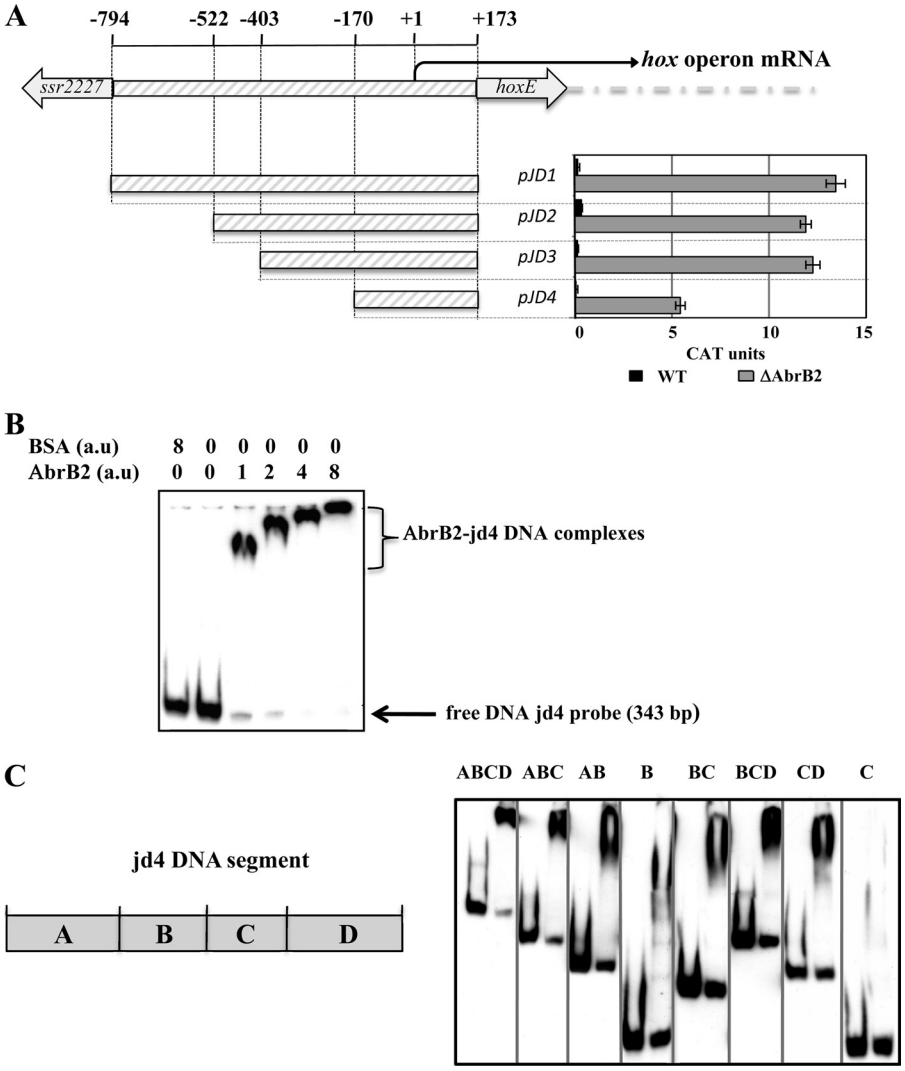

FIG 5 Analysis of the *hoxEFUYH* operon promoter through transcriptional fusion to the *cat* reporter gene and electrophoretic migration shift assay results for binding of the AbrB2 regulator. (A, top) Schematic representation of the *hoxEFUYH* operon promoter region (thick gray lines) located between the *hoxE* protein-coding sequence and the opposite (putative) transposase gene, ssr2227. The nucleotide positions within the *hoxEFUYH* operon promoter region are indicated relative to the transcription start site (bent arrow), taken as the origin of distance (noted as +1). For the sake of clarity, the operonic genes downstream of *hoxE* are indicated by the large dashed gray line. (A, bottom) Deletion analysis of the *hox* operon promoter region transcriptionally fused to the *cat* reporter gene of our replicative promoter probe vector. CAT specific activities driven by the resulting reporter plasmids replicating in *Synechocystis* WT or Δ*abrB2* (hatched gray bars) are expressed in nmol of chloramphenicol acetylated/min/mg of protein. They are the mean values ± standard deviations calculated from three independent experiments. (B and C) Analysis of the electrophoretic mobility of the DIG-labeled JD4 segment, or subsegments thereof, noted as A, B, C, and D, of the *hox* operon promoter, following incubation with increasing amounts of purified 6×His-AbrB2 regulator or the BSA negative-control protein. Arrows and braces indicate the positions of the free DNA probes and the retarded DNA-protein complexes, respectively.

pected, we identified a shorter *hox* regulatory region (343 bp; plasmid pJD4) that retained a promoter activity that was negatively regulated by the AbrB2 protein (i.e., higher in Δ*abrB2*::Km^r cells than WT cells) (Fig. 5A). Together, our data show that AbrB2 negatively regulates the expression of the *hox* operon at the level of its promoter activity.

AbrB2 represses expression of the *hox* operon through binding to its promoter and flanking regions. Using the suitably sized *hox* operon promoter region (343 bp; JD4 DNA) (Fig. 5A), we performed EMSAs to show that AbrB2 binds on the *hox* promoter region (Fig. 5B), as expected. The apparent size of the AbrB2-*hox* retardation complex appeared to increase in parallel with the increase in the molecular ratio of AbrB2 over *hox* DNA, indicating that several AbrB2 molecules can bind to each *hox* DNA molecule. As the usual controls for specific affinity of AbrB2 for *hox* DNA, we verified the absence of interaction between the *hox* DNA and the BSA control protein and that the abundance of the DIG-labeled *hox*-AbrB2 complex was decreased by the presence of an excess of unlabeled *hox* DNA (see Fig. S2 in the supplemental material).

We also tested the binding of AbrB2 on various segments of the 343-bp JD4 *hox* promoter region in an attempt to better localize the AbrB2-binding sites, and we named the segments A, B, C, and D for the sake of clarity. Fragment A (100 bp) is located upstream of fragment B (74 bp), which harbors the core promoter with the −35-like and −10-like boxes, followed by the downstream frag-

ments C (69 bp) and D (100 bp), in that order (Fig. 5C). We found that AbrB2 bound to all tested subregions, with the noticeable exception of fragment C alone (Fig. 5C). The occurrence of distant AbrB2-binding regions in the *hox* promoter regions suggests the possible involvement of a DNA looping mechanism in the AbrB2-mediated regulation of *hox* transcription.

DISCUSSION

It is important to thoroughly study the mechanisms controlling the expression of the cyanobacterial genes encoding the Ni-Fe bidirectional hydrogenase in order to better understand its role in the global metabolism of the cell and possibly generate new cell factories for better production of H_2. The pentameric hydrogenase Hox enzyme (HoxEFUYH) is mostly studied in the best-characterized cyanobacterium *Synechocystis* PCC6803. In *Synechocystis*, the five *hox* genes are grouped together with three genes of unknown function in an octacistronic "*hox*" operon (Fig. 4), which generates rare transcripts (5, 36). In the context of our long-term interest in gene expression, we decided to test whether this was due to the weak activity of the *hox* operon promoter. Therefore, we cloned the *hox* promoter region upstream of the promoterless *cat* reporter gene of our promoter probe plasmid vector, which replicates autonomously in *Synechocystis* at the same copy number as the chromosome (27). Our *hoxprom-cat* reporter plasmid (pJD1 [Fig. 5]) directed a very low level of *cat* expression in *Synechocystis* (less than 1 CAT unit), showing, for the first time, that the *hox* promoter is weakly active. This finding is at variance with the occurrence in the *hox* promoter of sequences resembling the canonical −35 (TTGctc) and −10 (TAacAa) promoter boxes (15, 35). Consequently, we speculated that the *hox* promoter might be controlled by a negative regulator. Hence, we became interested in the AbrB2 protein, which resembles the pleiotropic AbrB repressor of *B. subtilis* (6, 19). Working with the glucose-tolerant mutant of *Synechocystis*, which harbors several mutations with unknown physiological consequences (20), it was shown that the disruption of the sll0822 gene (here, *abrB2*) increased by about 2-fold the abundance of the *hox* transcripts monitored with DNA microarrays (19). Consequently, we decided to test the influence of AbrB2 on the expression and promoter activity of the *hox* operon. For this purpose, we used the wild-type strain of *Synechocystis*, because it is actually this strain that was originally isolated from nature. First, we deleted the *abrB2* gene from all copies of the *Synechocystis* chromosome, which is polyploid (13, 23), and we found that the corresponding mutant grew as well as the wild-type strain (Fig. 1). This result was similar, but not identical, to what was observed in the glucose-tolerant mutant, in which the inactivation of the *abrB2* gene strongly reduced the growth rate (19). This discrepancy might result from the differences in the strains (see above), growth conditions, and/or gene manipulation protocols employed by the two laboratories. While the previous workers introduced the Km^r marker inside the *abrB2*-coding sequence (at 177 bp downstream of the ATG start codon), which might thereby encode an aberrant protein impeding cell growth, we replaced the full *abrB2*-coding sequence with the Km^r marker to preclude the synthesis of AbrB2 (we have verified the absence of the *abrB2* gene [Fig. 1] and its transcripts [data not shown]).

Using our *abrB2*-deleted mutant, we verified through quantitative RT-PCR that the absence of AbrB2 increased (at least 2.5-fold) the transcript abundance of all eight genes of the *hox* operon (Fig. 4). In agreement, we showed, for the first time, that the amount of active hydrogenase was also increased (about 2-fold) in the absence of AbrB2 (Fig. 4). To confirm these findings, we constructed an *abrB2* overexpression mutant, by cloning the *abrB2* protein-coding sequence into our temperature-controlled expression vector, pFC1, which replicates autonomously in *Synechocystis* and strongly produces the studied protein after 24 h of induction at 39°C (32, 38). As expected, the resulting cells strongly expressed *abrB2* (27-fold more than noninduced cells) and concomitantly downregulated (at least 2-fold) *hox* expression and hydrogenase activity (Fig. 4). Furthermore, we showed that AbrB2 negatively regulated the activity of the *hox* promoter through binding to it (Fig. 5). Together, these novel findings demonstrate unambiguously that AbrB2 represses the *hox* operon. Furthermore, we found distant AbrB2-binding regions in the *hox* promoter region (Fig. 5), thereby suggesting the possible involvement of a DNA looping mechanism in the AbrB2-mediated repression of *hox* transcription. A similar hypothesis has been proposed for LexA-mediated regulation of the *hox* operon (36).

We also studied the expression and the regulation of the *abrB2* gene. First, we mapped its transcription start site (see Fig. S1 in the supplemental material), and we analyzed its promoter through mutations and transcriptional fusions to the promoterless *cat* reporter gene of our promoter probe plasmid vector (27). We report that *abrB2* is expressed from an atypical promoter harboring an extended −10 element (5′-TGTATAAT-3′) that compensates the absence of a −35 box (5′-TTGACA-3′) (Fig. 3), similarly to what we found previously for the *secA* gene (28). Confirming the biological significance of our results, we found the occurrence of an extended −10 promoter element and the absence of a −35 box to be two well-conserved features in the *abrB2* genes from various cyanobacteria (Fig. 3). Also, interestingly, we found the *abrB2* promoter to be about 3-fold more active in the *abrB2* deletion mutant (131 CAT units) than in the WT strain (44 units), thereby demonstrating that AbrB2 negatively regulates expression of its own gene. Furthermore, we verified through EMSA analysis (Fig. 2) that AbrB2 binds on its own promoter, in agreement with a previous observation (19). Collectively, our data demonstrate unambiguously that AbrB2 is an autorepressor that also represses the *hox* operon.

Finally, when looking for a DNA motif that occurs in the *abrB2* promoter and the *hox* promoter subfragments A, B, and D, which all bind AbrB2, but not in the C segment of the *hox* promoter, which does not bind AbrB2, we identified a consensus motif, TT(N_5)AAC, as being possibly involved in AbrB2 binding (see Fig. S2 in the supplemental material). In agreement with this hypothesis, the mutation of the TT(N_5)AAC motif (TTGAACAAAC to GGG AACAAAC), which overlaps the presumptive −35 box of the *abrB2* promoter, appeared to increase (not decrease) the activity of the *abrB2* promoter (Fig. 3).

We believe that our *abrB2*-deleted mutant with an improved hydrogenase activity and also our reporter plasmids for the analysis of the *abrB2* gene and *hox* operon in various host strains with relevant genetic backgrounds will help in deciphering the regulation and the function of the hydrogen production machine, so as to improve it.

ACKNOWLEDGMENTS

J.D. and P.S. were, respectively, recipients of Ph.D. and postdoctoral fellowships from the CEA (France). This work was supported by the

Agence Nationale de la Recherche Grants ANR-09-BIOE-002-01 (EngineeringH2cyano) and the CNRS (Centre National recherche scientifique) Programme Interdisciplinaire Energie PIE2 (Reprogramhydrogen), as well as the HélioBiotec platform, funded by the European Union, Région PACA, French Ministry of Research, and the CEA.

We thank Patrick Carrier and Pierre Richaud for their help in the MIMS analysis of the hydrogenase activity.

REFERENCES

1. **Abed RM, Dobretsov S, Sudesh K.** 2009. Applications of cyanobacteria in biotechnology. J. Appl. Microbiol. **106**:1–12.
2. **Angermayr SA, Hellingwerf KJ, Lindblad P, de Mattos MJ.** 2009. Energy biotechnology with cyanobacteria. Curr. Opin. Biotechnol. **20**:257–263.
3. **Aubert-Jousset E, Cano M, Guedeney G, Richaud P, Cournac L.** 2011. Role of HoxE subunit in *Synechocystis* PCC6803 hydrogenase. FEBS J. **278**:4035–4043.
4. **Barne KA, Bown JA, Busby SJ, Minchin SD.** 1997. Region 2.5 of the *Escherichia coli* RNA polymerase σ^{70} subunit is responsible for the recognition of the extended-10′ motif at promoters. EMBO J. **16**:4034–4040.
5. **Carrieri D, Wawrousek K, Eckert C, Yu J, Maness PC.** 2011. The role of the bidirectional hydrogenase in cyanobacteria. Bioresour. Technol. **102**: 8368–8377.
6. **Coles M, et al.** 2005. AbrB-like transcription factors assume a swapped hairpin fold that is evolutionarily related to double-psi beta barrels. Structure **13**:919–928.
7. **Cournac L, Guedeney G, Peltier G, Vignais PM.** 2004. Sustained photoevolution of molecular hydrogen in a mutant of *Synechocystis* sp. strain PCC 6803 deficient in the type I NADPH-dehydrogenase complex. J. Bacteriol. **186**:1737–1746.
8. **Deusch O, et al.** 2008. Genes of cyanobacterial origin in plant nuclear genomes point to a heterocyst-forming plastid ancestor. Mol. Biol. Evol. **25**:748–761.
9. **Domain F, Houot L, Chauvat F, Cassier-Chauvat C.** 2004. Function and regulation of the cyanobacterial genes *lexA*, *recA* and *ruvB*: LexA is critical to the survival of cells facing inorganic carbon starvation. Mol. Microbiol. **53**:65–80.
10. **Ducat DC, Way JC, Silver PA.** 2011. Engineering cyanobacteria to generate high-value products. Trends Biotechnol. **29**:95–103.
11. **Garcin P, et al.** 2012. A transcriptional-switch model for Slr1738-controlled gene expression in the cyanobacterium *Synechocystis.* BMC Struct. Biol. **12**:1. doi:10.1186/1472-6807-12-1.
12. **Ghirardi ML, Dubini A, Yu J, Maness PC.** 2009. Photobiological hydrogen-producing systems. Chem. Soc. Rev. **38**:52–61.
13. **Griese M, Lange C, Soppa J.** 2011. Ploidy in cyanobacteria. FEMS Microbiol. Lett. **323**:124–131.
14. **Grigorieva G, Shestakov S.** 1982. Transformation in the cyanobacterium *Synechocystis* sp. 6803. FEMS Microbiol. Lett. **13**:367–370.
15. **Gutekunst K, et al.** 2005. LexA regulates the bidirectional hydrogenase in the cyanobacterium *Synechocystis* sp. PCC 6803 as a transcription activator. Mol. Microbiol. **58**:810–823.
16. **Hawley DK, McClure WR.** 1983. Compilation and analysis of *Escherichia coli* promoter DNA sequences. Nucleic Acids Res. **11**:2237–2255.
17. **Heckman KL, Pease LR.** 2007. Gene splicing and mutagenesis by PCR-driven overlap extension. Nat. Protoc. **2**:924–932.
18. **Houot L, et al.** 2007. Cadmium triggers an integrated reprogramming of the metabolism of *Synechocystis* PCC6803, under the control of the Slr1738 regulator. BMC Genomics **8**:350. doi:10.1186/1471-2164-8-350.
19. **Ishii A, Hihara Y.** 2008. An AbrB-like transcriptional regulator, Sll0822, is essential for the activation of nitrogen-regulated genes in *Synechocystis* sp. PCC 6803. Plant Physiol. **148**:660–670.
20. **Kanesaki Y, et al.** 2012. Identification of substrain-specific Mutations by massively parallel whole-genome resequencing of *Synechocystis* sp. PCC 6803. DNA Res. **19**:67–79.
21. **Kiss E, Kos PB, Vass I.** 2009. Transcriptional regulation of the bidirectional hydrogenase in the cyanobacterium *Synechocystis* 6803. J. Biotechnol. **142**:31–37.
22. **Kruse O, Rupprecht J, Mussgnug JH, Dismukes GC, Hankamer B.** 2005. Photosynthesis: a blueprint for solar energy capture and biohydrogen production technologies. Photochem. Photobiol. Sci. **4**:957–970.
23. **Labarre J, Chauvat F, Thuriaux P.** 1989. Insertional mutagenesis by random cloning of antibiotic resistance genes into the genome of the cyanobacterium *Synechocystis* strain PCC 6803. J. Bacteriol. **171**:3449–3457.
24. **Lieman-Hurwitz J, et al.** 2009. A cyanobacterial AbrB-like protein affects the apparent photosynthetic affinity for CO2 by modulating low-CO2-induced gene expression. Environ. Microbiol. **11**:927–936.
25. **Liu X, Fallon S, Sheng J, Curtiss R III.** 2011. CO_2-limitation-inducible green recovery of fatty acids from cyanobacterial biomass. Proc. Natl. Acad. Sci. U. S. A. **108**:6905–6908.
26. **Maeda T, Sanchez-Torres V, Wood TK.** 2008. Metabolic engineering to enhance bacterial hydrogen production. Microb. Biotechnol. **1**:30–39.
27. **Marraccini P, Bulteau S, Cassier-Chauvat C, Mermet-Bouvier P, Chauvat F.** 1993. A conjugative plasmid vector for promoter analysis in several cyanobacteria of the genera *Synechococcus* and *Synechocystis.* Plant Mol. Biol. **23**:905–909.
28. **Mazouni K, Bulteau S, Cassier-Chauvat C, Chauvat F.** 1998. Promoter element spacing controls basal expression and light inducibility of the cyanobacterial *secA* gene. Mol. Microbiol. **30**:1113–1122.
29. **Mazouni K, Domain F, Cassier-Chauvat C, Chauvat F.** 2004. Molecular analysis of the key cytokinetic components of cyanobacteria: FtsZ, ZipN and MinCDE. Mol. Microbiol. **52**:1145–1158.
30. **McIntosh CL, Germer F, Schulz R, Appel J, Jones AK.** 2011. The [NiFe]-hydrogenase of the cyanobacterium *Synechocystis* sp. PCC 6803 works bidirectionally with a bias to H_2 production. J. Am. Chem. Soc. **133**:11308–11319.
31. **Mermet-Bouvier P, Cassier-Chauvat C, Marraccini P, Chauvat F.** 1993. Transfer and replication of RSF1010-derived plasmids in several cyanobacteria of the genera *Synechocystis* and *Synechococcus.* Curr. Microbiol. **27**:323–327.
32. **Mermet-Bouvier P, Chauvat F.** 1994. A conditional expression vector for the cyanobacteria *Synechocystis* sp. strains PCC6803 and PCC6714 or *Synechococcus* sp. strains PCC7942 and PCC6301. Curr. Microbiol. **28**:145–148.
33. **Mulkidjanian AY, et al.** 2006. The cyanobacterial genome core and the origin of photosynthesis. Proc. Natl. Acad. Sci. U. S. A. **103**:13126–13131.
34. **Oliveira P, Lindblad P.** 2008. An AbrB-Like protein regulates the expression of the bidirectional hydrogenase in *Synechocystis* sp. strain PCC 6803. J. Bacteriol. **190**:1011–1019.
35. **Oliveira P, Lindblad P.** 2005. LexA, a transcription regulator binding in the promoter region of the bidirectional hydrogenase in the cyanobacterium *Synechocystis* sp. PCC 6803. FEMS Microbiol. Lett. **251**:59–66.
36. **Oliveira P, Lindblad P.** 2009. Transcriptional regulation of the cyanobacterial bidirectional Hox-hydrogenase. Dalton Trans. **2009**: 9990–9996.
37. **Paumann M, Regelsberger G, Obinger C, Peschek GA.** 2005. The bioenergetic role of dioxygen and the terminal oxidase(s) in cyanobacteria. Biochim. Biophys. Acta **1707**:231–253.
38. **Poncelet M, Cassier-Chauvat C, Leschelle X, Bottin H, Chauvat F.** 1998. Targeted deletion and mutational analysis of the essential (2Fe-2S) plant-like ferredoxin in *Synechocystis* PCC6803 by plasmid shuffling. Mol. Microbiol. **28**:813–821.
39. **Rasmussen B, Fletcher IR, Brocks JJ, Kilburn MR.** 2008. Reassessing the first appearance of eukaryotes and cyanobacteria. Nature **455**:1101–1104.
40. **Rippka R, Deruelles J, Waterbury JB, Herdman M, Stanier RY.** 1979. Generic assignments, strains histories and properties of pure cultures of cyanobacteria. J. Gen. Microbiol. **111**:1–61.
41. **Schirmer A, Rude MA, Li X, Popova E, del Cardayre SB.** 2010. Microbial biosynthesis of alkanes. Science **329**:559–562.
42. **Scotto-Lavino E, Du G, Frohman MA.** 2006. Amplification of 5′ end cDNA with 'new RACE.' Nat. Protoc. **1**:3056–3061.
43. **Sheng J, Vannela R, Rittmann BE.** 2011. Evaluation of methods to extract and quantify lipids from *Synechocystis* PCC 6803. Bioresour. Technol. **102**: 1697–1703.
44. **Shi T, Falkowski PG.** 2008. Genome evolution in cyanobacteria: the stable core and the variable shell. Proc. Natl. Acad. Sci. U. S. A. **105**:2510–2515.
45. **Soni B, Houot L, Cassier-Chauvat C, Chauvat F.** 2012. Prominent role of the three *Synechocystis* PchR-like regulators in the defense against metal and oxidative stresses. Open J. Biochem. **1**:1. http://www.rossscience.org/ojbb/articles/2227-7021-1-1.htm.
46. **Sybirna K, et al.** 2008. Shewanella oneidensis: a new and efficient system for expression and maturation of heterologous [Fe-Fe] hydrogenase from *Chlamydomonas reinhardtii.* BMC Biotechnol. **8**:73. doi:10.1186/1472-6750-8-73.

47. **Tamagnini P, et al.** 2007. Cyanobacterial hydrogenases: diversity, regulation and applications. FEMS Microbiol. Rev. **31**:692–720.
48. **Wang R, Healey FP, Myers J.** 1971. Amperometric measurement of hydrogen evolution in chlamydomonas. Plant Physiol. **48**:108–110.
49. **Waterbury JB, Warson SW, Guillard RRL, Brand JE.** 1979. Widerspread occurrence of a unicellular, marine, planktonic, cyanobacterium. Nature **277**:293–294.
50. **Williams PG.** 2009. Panning for chemical gold: marine bacteria as a source of new therapeutics. Trends Biotechnol. **27**:45–52.
51. **Yamauchi Y, Kaniya Y, Kaneko Y, Hihara Y.** 2011. Physiological roles of the cyAbrB transcriptional regulator pair Sll0822 and Sll0359 in *Synechocystis* sp. strain PCC 6803. J. Bacteriol. **193**:3702–3709.
52. **Zehr JP.** 2011. Nitrogen fixation by marine cyanobacteria. Trends Microbiol. **19**:162–173.